Coherence versus radiance formulations of surface scattering

Brian G. Hoover
Advanced Optical Technologies, Albuquerque, NM, USA

Victor L. Gamiz
Air Force Research Laboratory, Directed Energy Directorate, Kirtland AFB, NM USA

ABSTRACT

Surface scattering can be formulated in terms of coherence functions averaged over surface realizations. The resulting integrals for the average scattered intensity are superficially similar to those derived in conventional formulations like the Kirchhoff, Beckmann, and physical-optics models, but the coherence function is subject to some essential conditions, which are extensions of previously-derived conditions on the radiometric parameters of primary, partially-coherent sources and their propagated fields, that significantly influence the resulting scattered-intensity or BRDF solutions. The field approximation that leads to conventional radiance-like models is compared to a field approximation that leads to a particular coherence model of surface scattering, which is reviewed and verified against radiometric and atomic-force microscope (AFM) data due to a standard diffuse-gold reflector, representing apparently the first verified inverse reflectance solution for a non-contrived diffuse rough surface.

Keywords: Scattering, surface roughness, coherence, radiometry, BRDF, AFM, diffuse-gold

1. INTRODUCTION

Polarization can be considered as a form of coherence. In 1954 Wolf introduced the *coherency matrix*, also known as the polarization matrix, which is largely interchangeable with the Stokes parameters and describes the polarization properties of beam-like electromagnetic fields at single points in space in terms of coherence among orthogonal vector field components.[1] Much more recently, Gori, Wolf, and others extended the description of random electromagnetic fields to unified theories of coherence and polarization,[2–4] utilizing the generally three-dimensional coherence matrix (in the space-time domain) and cross-spectral density matrix (in the space-frequency domain), the elements of which are functions of two points in space and time or frequency.

This paper presents the application of coherence theory to surface scattering. Since the resulting integrals for scattered intensity are superficially similar to those derived in conventional formulations like the Kirchhoff, Beckmann, and physical-optics models, which are here referred to as *radiance-like* models, the differences between coherence and radiance formulations are emphasized through examination of underlying scattered-field approximations. A recently-published coherence model of surface scattering,[5] based on a phase-screen approximation to the scattered surface field, is reviewed and applied to demonstrate a verifiably correct coherence solution for quasi-monostatic, ss-polarized laser reflectance from a diffuse-gold calibration standard. Surface parameters derived by inverting the coherence solution for the average scattered intensity are shown to agree with independent measurements from an atomic-force microscope (AFM), representing apparently the first verified inverse reflectance solution for a non-contrived diffuse rough surface.

While the treatment of this paper assumes the scalar-wave approximation, coherence formulations can be extended to electromagnetic waves, and hence draw upon unified theories of coherence and polarization,[2–4,6] through matrix formulations to be presented in subsequent papers.

Further author information: (Send correspondence to B.G.H.)
E-mail: hoover@advanced-optical.com, Telephone: 1 505 250 9586

Polarization Science and Remote Sensing III, edited by Joseph A. Shaw, J. Scott Tyo
Proc. of SPIE Vol. 6682, 66820H, (2007) · 0277-786X/07/$18 · doi: 10.1117/12.739232

2. SCATTERING AND COHERENCE

Here the average intensity scattered by a rough surface is cast in its conventional analytical form, which is compared to the conventional expression for radiant intensity from coherence theory. The similarities and differences between these expressions are determined by the approximation to the scattered surface field. Two common field approximations, the tangent-plane approximation and the phase-screen approximation, are reviewed in detail. It is shown that the tangent-plane approximation leads to radiance-like models while the phase-screen approximation can lead to a coherence model of surface scattering.

Referring to Fig. 1, if the quasi-monochromatic scalar field $u(\mathbf{x})$ (of center wavelength $\bar{\lambda}$) on the planar virtual surface S is known, the Helmholtz integral leads to the Rayleigh-Sommerfeld formula for the field at the point P as[7]

$$u(P) = \frac{j}{\bar{\lambda}} \iint_S u(\mathbf{x}) \frac{\exp(j\bar{k}r)}{r} \cos\theta d\mathbf{x}, \tag{2.1}$$

where $\mathbf{x} = x\hat{x} + y\hat{y}$ is the position vector over S, $\mathbf{r} = r\hat{r}$ is the vector from $\mathbf{x}$ to P, $\bar{k} = 2\pi/\bar{\lambda}$, and $\cos\theta = \hat{n} \cdot \hat{r}$, where $\hat{n}$ is a surface normal. Note S is a virtual surface just above the actual rough surface Σ. If the point P is in the far or Fraunhofer zone, the *speckle intensity* in the direction $\hat{s} = \bar{\mathbf{k}}_s/\bar{k}$ is expressible as

$$\begin{aligned} I(\bar{\mathbf{k}}_s) &= Z^2 u(P) u^*(P) \\ &= \frac{1}{\bar{\lambda}^2} \iint_{S_1} \iint_{S_2} u(\mathbf{x}_1) u^*(\mathbf{x}_2) \cos\theta_1 \cos\theta_2 \exp(-j\bar{\mathbf{k}}_s \cdot \boldsymbol{\Delta}\mathbf{x}) d\mathbf{x}_1 d\mathbf{x}_2, \end{aligned} \tag{2.2}$$

with $\boldsymbol{\Delta}\mathbf{x} = \mathbf{x}_1 - \mathbf{x}_2$.

As indicated schematically in Fig. 2, adding speckle intensities due to different realizations of the random surface averages-out the speckle, and what remains is the *average intensity*

$$\langle I(\bar{\mathbf{k}}_s) \rangle = \frac{1}{\bar{\lambda}^2} \iint_{S_1} \iint_{S_2} \langle u(\mathbf{x}_1) u^*(\mathbf{x}_2) \cos\theta_1 \cos\theta_2 \rangle \exp(-j\bar{\mathbf{k}}_s \cdot \boldsymbol{\Delta}\mathbf{x}) d\mathbf{x}_1 d\mathbf{x}_2 \tag{2.3}$$

in units of W/sr. The surface realizations are assumed to be independent and identically distributed (IID), although in practice this is almost never exactly true. If the surface field is a scattered *coherent* field, as from an incident laser beam, then the average intensity generally varies with the angle of incidence, through implicit dependence of $u(\mathbf{x})$ in Eq. 2.3, and is often called the *bidirectional reflectance distribution function (BRDF)*. Formally, the BRDF is the average intensity divided by the incident power and the cosine of the scattering angle. Equation 2.3 is nothing new–it represents nothing more than the application of established electrodynamic theorems and approximations. The entire problem still remains, that is, specifying the scattered surface field $u(\mathbf{x})$.

In order to relate the problem of surface scattering to coherence theory, we will call the correlation function in Eq. 2.3 Γ' :

$$\Gamma' \equiv \langle u(\mathbf{x}_1) u^*(\mathbf{x}_2) \cos\theta_1 \cos\theta_2 \rangle. \tag{2.4}$$

At this stage the $\cos\theta$ term is kept general, because it is interpreted differently in different field approximations. If Γ' satisfies the properties of a *coherence* function, then the integral for the average intensity,

$$\langle I(\bar{\mathbf{k}}_s) \rangle = \frac{1}{\bar{\lambda}^2} \iint_{S_1} \iint_{S_2} \Gamma'(\mathbf{x}_1, \mathbf{x}_2, \cos\theta_1, \cos\theta_2) \exp(-j\bar{\mathbf{k}}_s \cdot \boldsymbol{\Delta}\mathbf{x}) d\mathbf{x}_1 d\mathbf{x}_2 \tag{2.5}$$

is very similar to the integral for the *radiant intensity* $J(\bar{\mathbf{k}}_s)$ derived from coherence theory, which is

$$J(\bar{\mathbf{k}}_s) = \frac{\cos^2\theta_s}{\bar{\lambda}^2} \iint_{S_1} \iint_{S_2} \Gamma(\mathbf{x}_1, \mathbf{x}_2) \exp(-j\bar{\mathbf{k}}_s \cdot \boldsymbol{\Delta}\mathbf{x}) d\mathbf{x}_1 d\mathbf{x}_2, \tag{2.6}$$

where $\Gamma(\mathbf{x}_1, \mathbf{x}_2)$ is the *coherence function* on S, and θ_s is the scattering angle. Equation 2.6 is a cornerstone of optical coherence theory since the radiant intensity is a primary radiometric observable. Equations 2.5-2.6 suggest that if a correlation function Γ', defined by Eq. 2.4, could be found that satisfies the properties of a coherence function, then the resulting scattering model could be considered a coherence model, and many useful results from coherence theory could be applied to scattering analysis. Of course, it is the approximation to the scattered surface field $u(\mathbf{x})$ that determines whether or not Γ' qualifies as a coherence function.

2.1. Field Approximations

2.1.1. Tangent-Plane Approximation

The most popular approximation to the scattered surface field is the *tangent-plane approximation (TPA)*, developed in Beckmann's famous book on the topic.[8] The TPA says that light reflects from the actual surface Σ as if from a plane tangent to the actual surface at each point. Under the TPA $\cos\theta$ is interpreted as an *obliquity* factor, the projection of the normal to the actual surface onto the scattering direction. In general,

$$\begin{aligned} \cos\theta &= \hat{n} \cdot \hat{s} \\ &= -\sin\theta_s \sin\beta + \cos\theta_s \cos\beta, \end{aligned} \tag{2.7}$$

where $\beta \equiv \tan^{-1} m$ with m the surface slope. Assuming small slopes,[9]

$$\cos\theta \approx -m(\mathbf{x}) \sin\theta_s + \cos\theta_s. \tag{2.8}$$

Without loss of generality, for our purposes we assume a plane wave normally incident on a perfect conductor. In this case the TPA to the field on the actual surface Σ becomes

$$u_\Sigma(\mathbf{x}) = u_i \exp\left\{j\bar{k}h(\mathbf{x})\right\}, \tag{2.9}$$

where u_i is the incident field strength and h is the height function of the actual surface as denoted in Fig. 1. This field is transferred to the virtual surface S by the phase factor $\exp\left\{j\bar{k}h(\mathbf{x})\cos\theta_s\right\}$, ie,

$$\begin{aligned} u(\mathbf{x}) &= u_\Sigma(\mathbf{x}) \exp\left\{j\bar{k}h(\mathbf{x})\cos\theta_s\right\} \\ &= u_i \exp\left\{j\bar{k}h(\mathbf{x})(1+\cos\theta_s)\right\}. \end{aligned} \tag{2.10}$$

Therefore, under the TPA the correlation function in the scattering integral of Eq. 2.3 becomes

$$\begin{aligned} \Gamma'_{tp} &= u_i^2 \left\langle \left[m(\mathbf{x}_1) m(\mathbf{x}_2) \sin^2\theta_s - (m(\mathbf{x}_1) + m(\mathbf{x}_2)) \sin\theta_s \cos\theta_s + \cos^2\theta_s\right] \right. \\ &\quad \left. \times \exp\left\{j\bar{k}\left[h(\mathbf{x}_1) - h(\mathbf{x}_2)\right](1+\cos\theta_s)\right\}\right\rangle. \end{aligned} \tag{2.11}$$

The term in the slope m makes it nearly impossible to evaluate the TPA to the BRDF integral symbolically, so it's typically removed by invoking the *stationary-phase* approximation, in which case it becomes the deterministic function denoted by $F(\theta_i, \theta_s)$ and can be pulled outside of the integral. For normal incidence $F = 1$, which is assumed. Under this final approximation,

$$\Gamma'_{tp} = u_i^2 \left\langle \exp\left\{j\bar{k}\left[h(\mathbf{x}_1) - h(\mathbf{x}_2)\right](1+\cos\theta_s)\right\}\right\rangle \tag{2.12}$$

for normal incidence on a perfect conductor. Inserting this into the expression for the average intensity, Eq. 2.5,

$$\left\langle I\left(\bar{\mathbf{k}}_s\right)\right\rangle_{tp} = \frac{u_i^2}{\bar{\lambda}^2} \iint\limits_{S_1} \iint\limits_{S_2} \left\langle \exp\left\{j\bar{k}\left[h(\mathbf{x}_1) - h(\mathbf{x}_2)\right](1+\cos\theta_s)\right\}\right\rangle \exp\left(-j\bar{\mathbf{k}}_s \cdot \boldsymbol{\Delta}\mathbf{x}\right) d\mathbf{x}_1 d\mathbf{x}_2. \tag{2.13}$$

While certain of the preceding approximations can be avoided, and enhancements such as shadowing factors can be added, Eq. 2.13 represents the most common form of the family of scattering models known as Kirchhoff, Beckmann, or physical-optics models.

Comparing Eq. 2.13 with the radiant intensity of Eq. 2.6, we see that the TPA to the average intensity differs from the radiant intensity of coherence theory in two fundamental aspects. Firstly, the expressions disagree

in the $\delta-$*correlated* or *incoherent* limit, that is, as the correlation area of the scattered surface field becomes vanishingly narrow. This limit of the TPA to the average intensity is formally expressed as

$$\lim_{\gamma' \to \delta(\mathbf{\Delta x})} \left\langle I\left(\bar{\mathbf{k}}_s\right)\right\rangle_{tp} = \frac{\mathcal{A}u_i^2}{\bar{\lambda}^2}, \tag{2.14}$$

where γ' is the *normalized* correlation function and $\mathcal{A}$ is the illuminated area, while for the radiant intensity,

$$\lim_{\gamma \to \delta(\mathbf{\Delta x})} J\left(\bar{\mathbf{k}}_s\right) = \frac{\mathcal{A}\bar{I}\cos^2\theta_s}{\bar{\lambda}^2}, \tag{2.15}$$

where $\bar{I}$ is the average irradiance over the illuminated area. This disagreement apparently stems from the use of the stationary-phase approximation in the TPA. The stationary-phase approximation basically neglects diffraction, treating the surface as a collection of microfacets that reflect light geometrically, an approximation that should clearly break down as the correlation dimension becomes comparable to the wavelength. Problems with the TPA associated with the stationary-phase approximation, as manifest in Beckmann's model, have been demonstrated by other authors for surfaces far from the $\delta-$correlated limit.[10] These problems have been recognized and rectified by subsequent authors,[11] although with little physical justification.

The second disagreement between the TPA to the average intensity (Eq. 2.13) and the radiant intensity of coherence theory (Eq. 2.6) stems from the fact that Γ'_{tp} in Eq. 2.11 (and Eq. 2.12) is inadmissible as a coherence function because its associated correlation function depends on both of the conjugate variables $\mathbf{\Delta x}$ and θ_s. In this respect Γ'_{tp} has the properties of a *radiance* function, and therefore models that employ it are termed *radiance-like* models. It remains to be determined whether Γ'_{tp} can be classified as a *generalized radiance function,* ie, the result of a phase-space mapping of an operator derived from the coherence function Γ.[12] This disagreement provides much of the physical motivation for our study: in analogy with the principles of quantum mechanics, the form in which Γ'_{tp} depends on $\mathbf{\Delta x}$ and θ_s implies that it is non-measurable.[13,14]

2.1.2. Phase-Screen Approximation

In order to develop a coherence model of surface scattering it is apparently necessary to deviate from the most popular scattered-field approximation. One alternative, *the phase-screen approximation (PSA)*, was developed in Goodman's seminal work on statistical optics.[15] In Goodman's phase-screen approximation, the obliquity factor is that associated with the field on the virtual surface S, which is constant:

$$\cos\theta = \cos\theta_s. \tag{2.16}$$

The phase term due to the incident wave is the same as that under the TPA, Eq. 2.9 for a normally-incident plane wave, but the dependence of Γ' on the scattering direction is suppressed by assuming *no coherent phase relationships in the scattered field.* The scattered field is transferred from the actual surface Σ to the virtual surface S by the simple phase factor $\exp\left\{j\bar{k}h\left(\mathbf{x}\right)\right\}$, regardless of the incident angle. Thinking naively of geometrical propagation of partially-coherent waves, the PSA implies that the scattered wave propagates from Σ to S along trajectories normal to S. Then, for a plane wave normally incident on a perfect conductor the PSA to the scattered field becomes

$$u\left(\mathbf{x}\right) = u_i \exp\left\{2j\bar{k}h\left(\mathbf{x}\right)\right\}, \tag{2.17}$$

and the correlation function becomes

$$\Gamma'_{ps} = u_i^2\cos^2\theta_s\left\langle\exp\left\{2j\bar{k}\left[h\left(\mathbf{x}_1\right) - h\left(\mathbf{x}_2\right)\right]\right\}\right\rangle. \tag{2.18}$$

Finally, the PSA to the average intensity is

$$\left\langle I\left(\bar{\mathbf{k}}_s\right)\right\rangle_{ps} = \frac{u_i^2\cos^2\theta_s}{\bar{\lambda}^2}\iint\limits_{S_1}\iint\limits_{S_2}\left\langle\exp\left\{2j\bar{k}\left[h\left(\mathbf{x}_1\right) - h\left(\mathbf{x}_2\right)\right]\right\}\right\rangle\exp\left(-j\bar{\mathbf{k}}_s\cdot\mathbf{\Delta x}\right)d\mathbf{x}_1 d\mathbf{x}_2. \tag{2.19}$$

Comparison of Eq. 2.19 with Eq. 2.6 reveals that the PSA leads to a coherence model of surface scattering provided that

$$u_i^2\left\langle\exp\left\{2j\bar{k}\left[h\left(\mathbf{x}_1\right) - h\left(\mathbf{x}_2\right)\right]\right\}\right\rangle = \Gamma\left(\mathbf{x}_1, \mathbf{x}_2\right), \tag{2.20}$$

that is, provided that the left-hand side of Eq. 2.20 qualifies as a coherence function. Since the correlation function associated with Γ'_{ps} depends only on $\mathbf{\Delta x}$ and not on θ_s, Eq. 2.20 can generally be satisfied. A particular example, with a Gaussian-distributed height function h, was demonstrated by Goodman[15] and leads to the coherence model reviewed in the following section.

2.2. A Coherence Model of Surface Scattering

Here we briefly review a coherence model of surface scattering we have developed based on Goodman's PSA to the scattered surface field. Readers are referred to our previous paper for details.[5] This model assumes a Gaussian distribution of surface heights, although the approach should be applicable to other height distributions. While the model will be generalized in subsequent versions, the current version assumes a scalar incident wave reflected by a perfectly-conducting surface, which implies that it should be more accurate in predicting the electromagnetic scattered field component perpendicular to the incident plane (*s polarization*) than the component parallel to the incident plane (*p polarization*), a limitation incorporated into the results presented in Section 3. The model assumes that the surface roughness is comparable to or larger than the illumination wavelength, ie, $\sigma \equiv \sigma_h/\bar{\lambda} \gtrsim 1$, (and/) *or* that the surface autocorrelation function is approximately quadratic, a union of conditions that dramatically expands its range of applicability. In the current version the normalized model solutions are functions of three surface parameters: the standard deviation of the surface height distribution, ie, the *roughness* σ_h, and the first two derivatives of the surface autocorrelation function evaluated at the origin, which are denoted by ρ_1 and ρ_2. The general quadratic expansion of the surface autocorrelation function leads to BRDF solutions that smoothly interpolate between the well-known results of the linear and parabolic approximations, ie, the Cauchy and Gaussian BRDFs, respectively. The model is not subject to any limitation on surface slopes–infinite slopes in fact lead to the Cauchy BRDF solution–although shadowing and multiple scattering are excluded from the current version. The final model expression for the average scattered intensity comprises an incoherent term plus an integral of the plasma dispersion function over a line in the complex plane. Computations of bistatic specular-plane average scattered intensity with $\pi/100$ angular resolution take approximately 30s in Mathematica 5 running under the Windows XP operating system on a 1.6GHz Intel Pentium 4 Mobile CPU with 512MB RAM.

3. RESULTS

This section summarizes the results of a case study of the coherence model described above[5] applied to data due to a standard diffuse-gold reflector. The model solution for average scattered intensity is fit to measured radiometric data, and the surface parameters that produce the model solution are verified against independent measurements of the surface made by an atomic-force microscope (AFM). To our knowledge this represents the first verified inverse reflectance solution for a non-contrived diffuse rough surface, "non-contrived" meaning that the statistical parameters of the surface were *not* designed to satisfy the assumptions of the model. This section summarizes the preliminary results of the study. Details and optimized results will appear in a follow-up paper.

The components of the case study include

(a) Flat-plate diffuse-gold reflector, manufactured by Epner. This reflector material is a common coating for integrating spheres and other IR instrumentation;

(b) Measured radiometric data: quasi-monostatic, ss-polarized BRDF at $\bar{\lambda} = 1.06\mu m$, measured at AFRL/DE. For these measurements the TEM_{00} probe spot was 5mm in diameter and the bistatic angle fixed at 2°. For preliminary model fits the data is shifted by 2° and compared with the true monostatic model solution;

(c) The coherence BRDF model described in Section 2.[5] The key features of the model for this study are invertibility in terms of measurable surface parameters $(\sigma_h, \rho_1, \rho_2)$ and accurate description of the relevant reflectance phenomenology;

(d) AFM surface data: $50 \times 50\mu m$ scan area with $.14nm$ vertical (height) resolution and $50nm$ horizontal resolution, measured at AFRL/DE on a Quesant AFM. Details of parameter extraction from the AFM data will appear in a follow-up paper.

The surface parameters extracted from the AFM data are used to seed a coarse optimization routine that results in the model fit reproduced in Fig. 3. The surface parameters that generate the model curve in Fig. 3 are within 20% of the parameters extracted from the AFM data. The surface autocorrelation coefficients are approximately equal, ie, $\rho_1 \approx \rho_2$, which implies that the autocorrelation function is strongly non-Gaussian. The fit is extremely good over a 150° elevation range and two orders of magnitude. In the monostatic geometry the ranges of both the incident and scattering angles are $\left[\begin{array}{cc} -75^\circ & 75^\circ \end{array} \right]$. An ideal Lambertian curve is included in Fig. 3 as a reference.

4. CONCLUSIONS

This paper attempts to emphasize some fundamental differences between coherence and radiance formulations of surface scattering. Field approximations under the two categories and a recently-published coherence model of surface scattering are reviewed. Despite the simplicity of the phase-screen approximation used to derive the coherence model, the accuracy and physical-realism of the model are verified through comparison with a limited radiometric data set and independent AFM data due to a standard diffuse-gold reflector. Comparable verified inverse solutions for non-contrived diffuse reflectors have not been found in the 50+ years worth of literature on radiance-like reflectance models.

ACKNOWLEDGMENTS

The authors thank David Medina, Nick Morley, and Stan Peplinski at AFRL/DE, David Reicher at S-Systems for AFM support, and Alan Ames, Ralph Cover, and Shawn Gay at Ball SES for analysis support.

REFERENCES

1. E. Wolf, "Optics in terms of observable quantities," Nuovo Cimento **12**, 884 (1954).
2. F. Gori, "Matrix treatment for partially polarized, partially coherent beams," Opt. Lett. **23**, 241-243 (1998).
3. E. Wolf, "Unified theory of coherence and polarization of random electromagnetic beams," Phys. Lett. A **312**, 263-267 (2003).
4. J. Tervo, T. Setälä, and A. T. Friberg, "Degree of coherence of electromagnetic fields," Opt. Exp. **11**, 1137-1142 (2003).
5. B. G. Hoover and V. L. Gamiz, "Coherence solution for bidirectional reflectance distributions of surfaces with wavelength-scale statistics," J. Opt. Soc. Am. A **23**(2), 314-328 (2006).
6. O. Korotkova, B. G. Hoover, V. L. Gamiz, and E. Wolf, "Coherence and polarization properties of far fields generated by quasi-homogeneous planar electromagnetic sources," J. Opt. Soc. Am. A **22**(11), 2547-2556 (2005).
7. J. W. Goodman, *Introduction to Fourier Optics*, 2nd. ed. (McGraw-Hill, New York, 1996), Chap. 3.
8. P. Beckmann and A. Spizzichino, *The Scattering of Electromagnetic Waves from Rough Surfaces* (Pergamon Press, New York, 1963).
9. For numerical solutions the small-slope approximation can be avoided. See N. C. Bruce, "Scattering from infinitely sloped surfaces by use of the Kirchhoff approximation," Appl. Opt. **42**(13), 2398 (2003).
10. K. A. O'Donnell and E. R. Méndez, "Experimental study of scattering from characterized random surfaces," J. Opt. Soc. Am. A **4**(7), 1194-1205 (1987).
11. J. E. Harvey, C. L. Vernold, A. Krywonos, and P. L. Thompson, "Diffracted radiance: a fundamental quantity in nonparaxial scalar diffraction theory," Appl. Opt. **38**(31), 6469 (1999).
12. G. S. Agarwal, J. T. Foley, and E. Wolf, "The radiance and phase-space representations of the cross-spectral density operator," Opt. Commun. **62**(2), 67-72 (1987).
13. E. Wolf, "Coherence and radiometry," J. Opt. Soc. Am. **68**(1), 7-17 (1978).
14. A. T. Friberg, "Effects of coherence in radiometry," Opt. Eng. **21**, 927-936 (1982); *Selected Papers on Coherence and Radiometry*, A. T. Friberg, ed., SPIE Milestone Series **69** (SPIE Optical Engineering Press, Bellingham, 1993).
15. J. W. Goodman, "Statistical Properties of Laser Speckle Patterns," in *Laser Speckle and Related Phenomena,* 2nd enlarged ed., J. C. Dainty, ed. (Springer-Verlag, Berlin, 1984), Chap. 2.

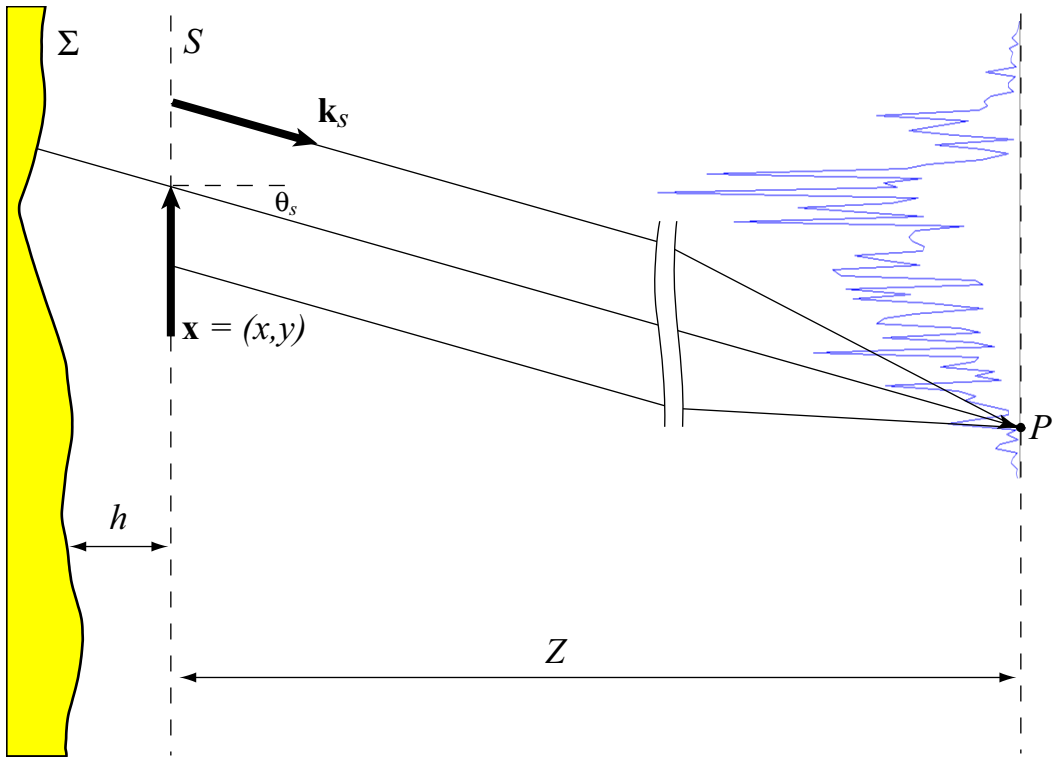

Figure 1. Conventional geometry and notation for expression of scattered radiometric observables. The surface representations Σ in Figures 1-2 are 30μm segments of actual AFM profiles of the diffuse-gold surface examined in Section 3, with a length:height (*h*) aspect ratio of 2:1.

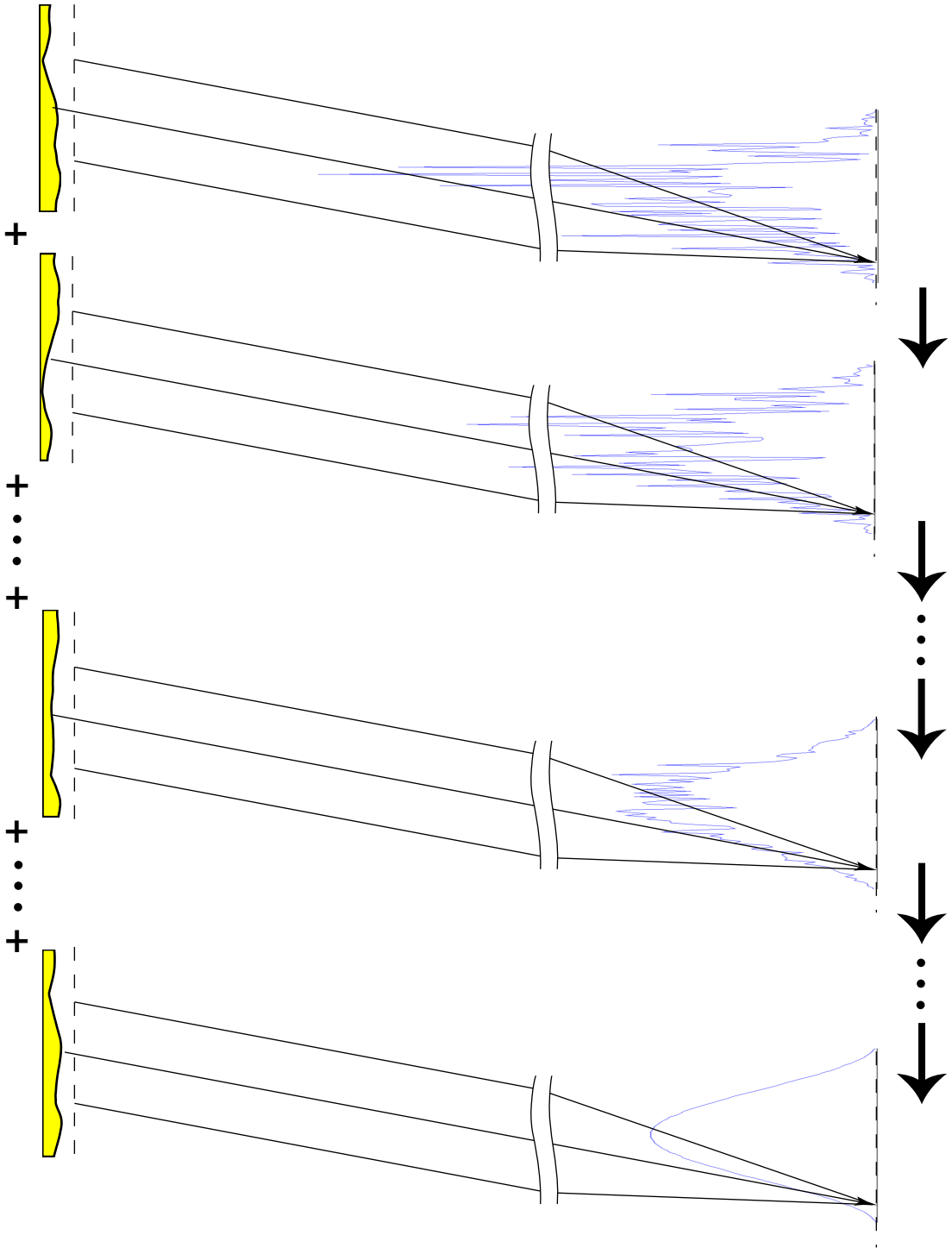

Figure 2. Schematic of speckle averaging. Speckle variations average out in the normalized integrated intensity as more surface realizations are illuminated. The surface representations Σ in Figures 1-2 are 30μm segments of actual AFM profiles of the diffuse-gold surface examined in Section 3, with a length:height (*h*) aspect ratio of 2:1.

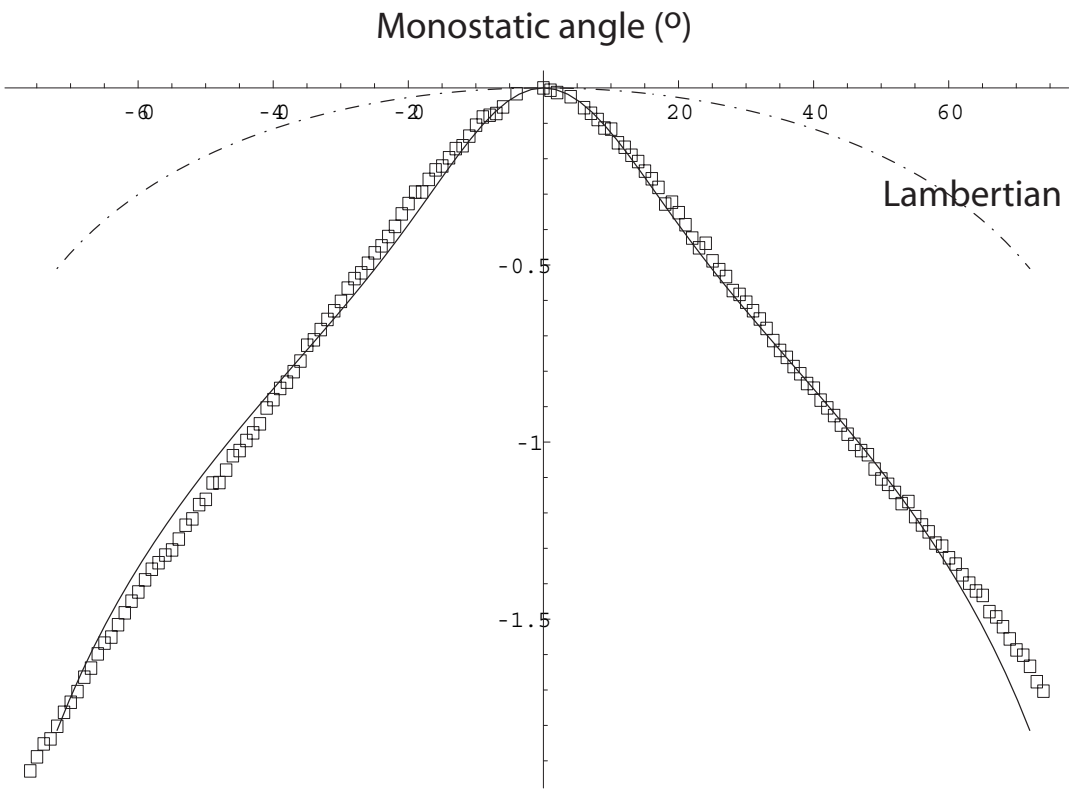

Figure 3. Coherence model fit (—) to ss-polarized quasi-monostatic average-intensity data ($\lambda = 1.06\mu m$) due to a diffuse-gold reflector (□). An ideal Lambertian intensity is shown for comparison.